

Applications and properties of the Bijvoet intensity ratio

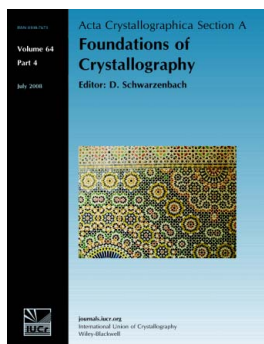
H. D. Flack and G. Bernardinelli

Acta Cryst. (2008). **A64**, 484–493

Copyright © International Union of Crystallography

Author(s) of this paper may load this reprint on their own web site or institutional repository provided that this cover page is retained. Republication of this article or its storage in electronic databases other than as specified above is not permitted without prior permission in writing from the IUCr.

For further information see <http://journals.iucr.org/services/authorrights.html>



Acta Crystallographica Section A: Foundations of Crystallography covers theoretical and fundamental aspects of the structure of matter. The journal is the prime forum for research in diffraction physics and the theory of crystallographic structure determination by diffraction methods using X-rays, neutrons and electrons. The structures include periodic and aperiodic crystals, and non-periodic disordered materials, and the corresponding Bragg, satellite and diffuse scattering, thermal motion and symmetry aspects. Spatial resolutions range from the subatomic domain in charge-density studies to nanodimensional imperfections such as dislocations and twin walls. The chemistry encompasses metals, alloys, and inorganic, organic and biological materials. Structure prediction and properties such as the theory of phase transformations are also covered.

Crystallography Journals **Online** is available from journals.iucr.org

Applications and properties of the Bijvoet intensity ratio

H. D. Flack* and G. Bernardinelli

Laboratoire de Cristallographie, University of Geneva, Switzerland. Correspondence e-mail: howard.flack@unige.ch

An empirical relationship of use in prediction and evaluation is established between the standard uncertainty of the Flack parameter and the Bijvoet intensity ratio. The expected value of this ratio may be calculated from the chemical composition of the compound and the X-ray wavelength. Structure analyses published with intensity data have allowed various properties of the Bijvoet intensity ratio to be studied. It is found that, although the Bijvoet intensity ratio has a strong dependence on $\sin \theta/\lambda$, extrapolation to $\sin \theta/\lambda = 0$ of model intensity pairs leads to values satisfactorily close to those expected. Moreover, it is shown that there is no symmetry enhancement for general reflections of the Bijvoet ratio in agreement with theory. The behaviour of some special reflections is examined. Two methods of correcting the observed Bijvoet ratio for systematic and random effects have been tested and found to be unsatisfactory. Evidence is produced to show that standard uncertainties provided with intensities are unrealistic and that measurement protocols need improvement.

© 2008 International Union of Crystallography
Printed in Singapore – all rights reserved

1. Introduction

Flack & Shmueli (2007) presented the theoretical derivation of the mean-square Friedel intensity difference in triclinic space group $P1$ with a centrosymmetric substructure and further defined a Bijvoet intensity ratio as the quotient of the root-mean-square Friedel intensity difference to the average reflection intensity. An expected value of the Bijvoet intensity ratio may be calculated from knowledge of the chemical composition of the compound and the X-radiation used. If it is required to make allowance for a centrosymmetric substructure, the chemical composition of the latter must also be known. Shmueli *et al.* (2008) have extended the analysis to all non-centrosymmetric space groups and have evaluated the symmetry-enhancing effects on the intensity of special reflections.

Previously, Flack *et al.* (2006) made a preliminary presentation for some crystal-structure determinations of the relationship between the Bijvoet ratio and the standard uncertainty (u) of the Flack (1983) parameter $x(u)$ obtained by least-squares refinement. However, the work presented in Flack *et al.* (2006) was limited in certain respects. In the first place, only an approximate form of the expected Bijvoet ratio due to Girard *et al.* (2003) was used and, secondly, the analysis was based on a small set of pseudo-centrosymmetric structures. Consequently, the current work presents the full relationship between the expected value of the Bijvoet ratio and the standard uncertainty of the Flack parameter, and moreover probes more deeply the practical properties of the Bijvoet ratio.

As in Flack & Shmueli (2007), we define the average and difference intensities of Friedel opposites as

$$A(hkl) = \frac{1}{2}[I(hkl) + I(\bar{h}\bar{k}\bar{l})], \quad (1)$$

$$D(hkl) = I(hkl) - I(\bar{h}\bar{k}\bar{l}) \quad (2)$$

and the Bijvoet intensity ratio is defined as

$$\chi = \sqrt{\langle D^2 \rangle} / \langle A \rangle. \quad (3)$$

The expected value of the Bijvoet intensity ratio χ_{Ex} is calculated using equation (8) of Flack & Shmueli (2007). For convenience, we use $10^4 \chi_{\text{Ex}}$, which is called *Friedif* for an arrangement without any centrosymmetric substructure and *Friedif-centro* if there is a centrosymmetric substructure. $Friedif \geq Friedif\text{-centro} \geq 0.0$. For a centrosymmetric structure, $Friedif = 0$.

According to the symmetry of the crystal, reflections are classified as being *general* or *special* and *centric* or *acentric*. These terms are rigorously defined with examples in Shmueli *et al.* (2008). A glossary is provided at the end of the current paper collecting the principal symbols used.

2. Application relating the standard uncertainty of the Flack parameter to *Friedif*

The various data sources that have been used for the study of the relationship between the standard uncertainty of the Flack parameter, u , and *Friedif* are given in Table 1. Data on crystal-structure analyses have been assigned a unique code SFA to

Table 1

Data sources for the study of the standard uncertainty of the Flack parameter *versus* Bijvoet intensity ratio.

Structure ATOTOS ($Friedif = 1171$, $u = 0.33$, $u.Friedif = 387$) in data set NiD clearly has something wrong in its reporting and has not been counted in the averages. Structure DAFPAC ($Friedif = 242$, $u = 0.08$, $u.Friedif = 19.4$) has been confirmed by the authors (Clemente, 2007) to be centrosymmetric but has been kept in data set PaD as originally published. Fuller information on these structures and the interpretation of their data is available from the supplementary material.

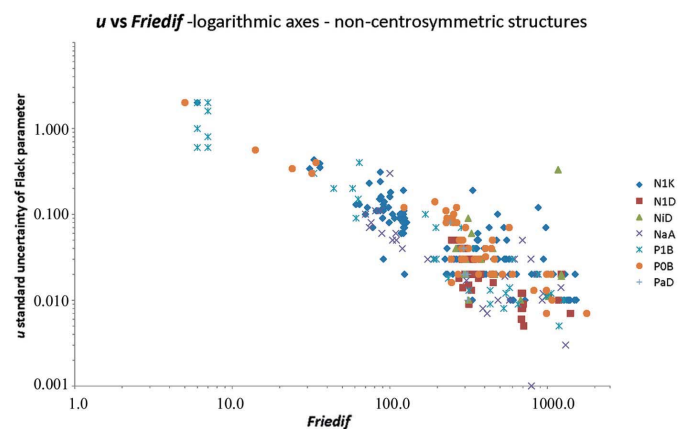
SFA code	Count	$\langle u.Friedif \rangle$	Centro-symmetry	% Friedel cover	Author
N1K	148	13.9	Non	100	This work
N1D	50	8.4	Non	100	Djukic <i>et al.</i> (2008)
NiD	16	13.6	Non	Intermediate	Djukic <i>et al.</i> (2008)
NaA	30	9.6	Non	Any	This work, Table 3
P1B	36	10.2	Pseudo	100	Flack <i>et al.</i> (2006)
P0B	50	14.7	Pseudo	0	Flack <i>et al.</i> (2006)
PaD	6	8.7	Pseudo	Any	Djukic <i>et al.</i> (2008)
C1B	30	25.9	Centro	100	Flack <i>et al.</i> (2006)
COB	66	23.1	Centro	0	Flack <i>et al.</i> (2006)
CIb	10	32.7	Centro	Intermediate	Flack <i>et al.</i> (2006)
C1X	5	2899.5	Centro	100	Flack <i>et al.</i> (2006, §5)

aid in identification. The code S takes a value of N to indicate a non-centrosymmetric structure without any centrosymmetric substructure, a value of P to indicate a non-centrosymmetric structure with a centrosymmetric substructure, and a value of C for a centrosymmetric structure which was (incorrectly) refined as being non-centrosymmetric. F indicates the Friedel coverage¹ of the intensity data as 0 for 0%, 1 for 100%, i (intermediate) for between 30 and 70%, and a (any) for any Friedel coverage noting that centric reflections do not count in this evaluation. The single-character A is a code indicating the source of the data, *e.g.* D means Djukic *et al.* (2008) as indicated in Table 1. Structures in data set N1K, which were obtained over a long period of time using various equipment and measurement procedures, have been marked as non-centrosymmetric since no centrosymmetric substructures were noticed and remarked upon at the time of the structure analysis when automated procedures like checkCIF/PLATON (<http://checkcif.iucr.org>; Spek, 2003) were not available and graphic display was less professional.

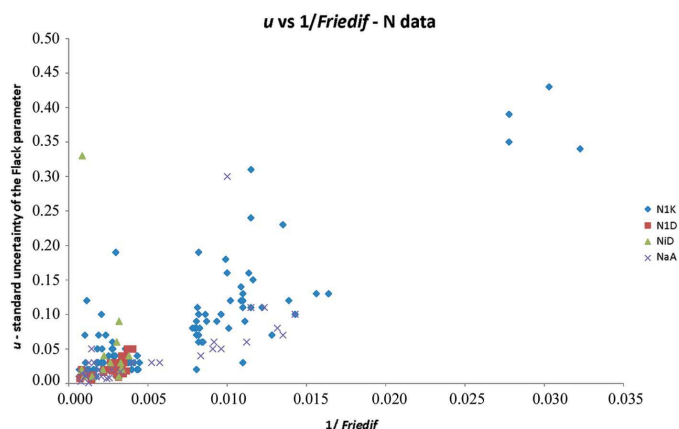
For much of the above data, the values obtained for the Flack parameter itself [*i.e.* the x in $x(u)$] have been extensively analysed and discussed in Flack & Bernardinelli (2006), Flack *et al.* (2006) and Djukic *et al.* (2008). In the current section, we are almost exclusively concerned with the value of the standard uncertainty of the Flack parameter [*i.e.* the u in $x(u)$] and in particular its relation to *Friedif*.

Fig. 1 shows the scatter diagram of u versus *Friedif* on logarithmic axes for the data sets of non-centrosymmetric and

pseudo-centrosymmetric crystal structures detailed in Table 1. The justification for incorporating the latter with those not containing a centrosymmetric substructure is presented in §2.1 following a consideration of the results on centrosymmetric structures. Although there is a fair amount of scatter of the data points in Fig. 1, several aspects are clear in it. Firstly, there is no grouping of data points based on Friedel coverage. Thus, for the purposes of the analysis of the standard uncertainty of the Flack parameter, data sets with large and small Friedel coverage may be treated together. Nevertheless, one should remember from Flack *et al.* (2006) that the value of x itself is sensitive to Friedel coverage. Secondly, it is clear that the data show an empirical linear relationship $\log(u) = m \log(Friedif) + \log(c)$. The important salient feature of this plot is that the slope m is essentially equal to -1 , giving $u = c/Friedif$, showing that u is inversely proportional to *Friedif* with the mean value of $u.Friedif$ (*i.e.* $\langle u.Friedif \rangle$) taken over a data set being an empirical constant. As an illustration, Fig. 2 shows the

**Figure 1**

Plot of u versus *Friedif* on logarithmic axes for non-centrosymmetric structures. These are measured with high and low Friedel coverage and may have a centrosymmetric substructure.

**Figure 2**

Plot of u versus $1/Friedif$ for non-centrosymmetric structures lacking a centrosymmetric substructure. Structure BU/17/611 ($Friedif = 6$, $u = 2.0$, $u.Friedif = 12.0$) in data set N1K has not been included in this figure as although its behaviour is normal it makes the scatter diagram less informative.

¹ Friedel coverage is a measure of the completeness of the diffraction-intensity data with regard to inversion in the origin of reciprocal space. If for each value of hkl the intensity of the Friedel opposite $\bar{h}\bar{k}\bar{l}$ (or one symmetry equivalent to it) has NOT been measured, then the Friedel coverage is 0%. However, if, for each value of hkl , both the reflection hkl and its Friedel opposite $\bar{h}\bar{k}\bar{l}$ (or one symmetry equivalent to it) have been measured and used separately in the least-squares refinement, then the Friedel coverage is 100%. Centric reflections do not count in this evaluation.

nice scatter diagram of u versus $1/\text{Friedif}$ for the non-centrosymmetric structures lacking a centrosymmetric substructure and Table 1 shows values of $\langle u.\text{Friedif} \rangle$ of 13.9 (N1K), 8.4 (N1D), 13.6 (NiD) and 9.6 (NaA). The spread of $u.\text{Friedif}$ values is best judged by examination of Figs. 1, 2 and 3, and by the spread of $\langle u.\text{Friedif} \rangle$ between data sets.

Using $\langle u.\text{Friedif} \rangle = 8.0$, one finds that $u = 0.04$ corresponds to a value for Friedif of 200 and a value of $u = 0.10$ corresponds to a value for Friedif of 80. These two values of u are the limiting values chosen by Flack & Bernardinelli (2000) as upper limits for absolute-structure determination: $u = 0.04$ for the general case and $u = 0.10$ for a compound known to be enantiopure. Consequently, the corresponding values of Friedif (200 for general and 80 for enantiopure) are lower limits for absolute-structure determination calculable from a knowledge of the chemical composition of the compound and the wavelength of the X-rays. These two values are thus of practical use in the choice of compound and radiation wavelength for absolute-configuration determination prior to experimentation and in the evaluation of the value of u obtained (see §2.2 for examples). The present Fig. 1 with its derived values supersedes Fig. 1 of Flack *et al.* (2006).

2.1. Centrosymmetric structures

Fig. 3 shows data for centrosymmetric structures supplementing the non-centrosymmetric structures already shown in Fig. 2. The scales of the two figures are not identical, details being given in the figure captions. Once again, the Friedel coverage has no clear effect on the value of u as all data sets of centrosymmetric structures occupy the same part of the scatter diagram. It is however very clear that the data points of the centrosymmetric structures tend to occur with a higher value of u , for a given value of Friedif , than those of non-centrosymmetric structures. Indeed, Table 1 shows values of $\langle u.\text{Friedif} \rangle$ for the centrosymmetric structures of 25.9 (C1B),

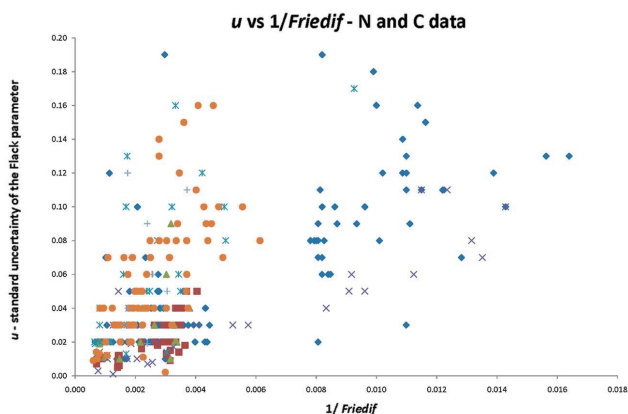


Figure 3
Plot of u versus $1/\text{Friedif}$ for centrosymmetric structures and non-centrosymmetric structures lacking a centrosymmetric substructure. Data with $u > 0.2$ have been excluded from the figure as although their behaviour is normal their inclusion makes the scatter diagram less informative. Consequently, Figs. 2 and 3 are not on the same scale.

Table 2
Examples of values of Friedif .

Compound	Friedif (Mo $K\alpha$)	Friedif (Cu $K\alpha$)
$\text{C}_{35}\text{H}_{36}\text{FeO}_2\text{P}$	405	1520
$\text{C}_{49}\text{H}_{27}\text{ClF}_{20}\text{O}_4\text{P}_2\text{Ru}$	232	904
$\text{C}_{20}\text{H}_{16}\text{CrO}_6$	342	1328
$\text{C}_{14}\text{H}_{17}\text{NO}_2\text{S}$	92	411
$\text{C}_6\text{H}_{12}\text{O}_6$	7	36

23.1 (C0B), 32.7 (CiB) and 2900 (C1X). The first three data sets imply that on average the values of Friedif for these centrosymmetric structures should be reduced by a factor of about 0.33 to bring them into line with the non-centrosymmetric structures. The analysis of Flack & Shmueli (2007) shows that the value of Friedif is decreased in the presence of a centrosymmetric substructure for a structure in triclinic space group $P1$. Thus, although it is encouraging to see that these data sets indicate that reduced values of Friedif are in operation, it may appear odd that the theoretical values of Friedif (*i.e.* zero) and u (*i.e.* infinitely large) for a centrosymmetric structure have not been attained. However, one has to recall that, although the real crystals of these compounds are centrosymmetric, the models used to represent them are non-centrosymmetric. In this respect, the well established instability of least-squares refinement of pseudo-centrosymmetric structures is of importance (Ermer & Dunitz, 1970; Marsh, 1981, 1986; Watkin, 1994). The freedom offered to a centrosymmetric crystal structure of a non-centrosymmetric least-squares refinement results in a better statistical fit to the intensity data at the expense of distorted molecular geometry and a physically unrealistic non-centrosymmetric distortion to the whole structure. Certain other factors also give rise to underestimated values of u . These are non-full-matrix least-squares refinement (Flack & Bernardinelli, 2000, 2006), the use of shift-limiting constraints (Watkin, 1994) and the Levenberg–Marquardt stabilizing or damping procedure (Levenberg, 1944; Marquardt, 1963; Flack & Bernardinelli, 2000).

The data set C1X of five crystal structures discussed in §5 of Flack *et al.* (2006) show large standard uncertainties u on the Flack parameter. All of these structures have a checkCIF/*PLATON* misfit parameter (Spek, 2003) to a centrosymmetric structure of 100%. The values of $u.\text{Friedif}$ for these structures are indeed so high, 5000, 5110, 226, 42 and 4120, that they have not been included in Fig. 3.

As promised at the start of §2, we now return to the examination of non-centrosymmetric crystal structures with a centrosymmetric substructure. In Fig. 1, it was seen that the corresponding data sets followed the same general trend as the data sets of non-centrosymmetric crystal structures without a centrosymmetric substructure. Moreover, for the data sets of pseudo-centrosymmetric crystal structures, $\langle u.\text{Friedif} \rangle$ takes values of 10.2 (P1B), 14.7 (P0B) and 8.7 (PaD), very similar to those of the data sets of non-centrosymmetric crystal structures without a centrosymmetric substructure. All in all, both the form of Flack & Shmueli's χ

and the freedom of a non-centrosymmetric refinement for the centrosymmetric substructure combine to make the effect of the centrosymmetric substructure minimal for the analysis of u in terms of *Friedif*.

2.2. Examples

A few examples presented in Table 2 will help to make some of the uses of *Friedif* clearer. In Table 2, one notices that the compound containing the heaviest element (Ru) is not the one with the highest value of *Friedif* and that the compound $C_{14}H_{17}NO_2S$ containing only elements from the first two rows of the Periodic Table nevertheless has significant and measurable differences in intensity between Friedel opposites even for Mo $K\alpha$. The compound $C_6H_{12}O_6$ has small differences in intensity between Friedel opposites with Mo $K\alpha$ radiation which increase on using Cu $K\alpha$ and are appreciable with Cr $K\alpha$ (*Friedif* = 80). If the above compounds have non-centrosymmetric crystal structures, on using the criteria established above in §2, we see that it should be possible to determine the absolute structure with either Mo $K\alpha$ or Cu $K\alpha$ radiation for $C_{35}H_{36}FeO_2P$, $C_{49}H_{27}ClF_{20}O_4P_2Ru$, $C_{20}H_{16}CrO_6$ and $C_{14}H_{17}NO_2S$ (Cu $K\alpha$ only). In these cases, an absolute-configuration determination is possible if all of the supplementary conditions described by Flack & Bernardinelli (1999, 2000, 2008) hold. Supposing the compounds $C_{14}H_{17}NO_2S$ and $C_6H_{12}O_6$ are known to be enantiopure, an absolute-configuration determination may be undertaken with either Mo $K\alpha$ or Cu $K\alpha$ radiation for $C_{14}H_{17}NO_2S$, whereas for $C_6H_{12}O_6$ this cannot be achieved with Mo $K\alpha$ and probably only with non-standard intensity measurements using Cu $K\alpha$ or Cr $K\alpha$.

Turning to the use of *Friedif* in the evaluation of published crystal structures, it seems reasonable from the results of §2.1 to treat values of u .*Friedif* greater than 25 as very suspicious. They may well indicate that the crystal structure is centrosymmetric or contains a significant centrosymmetric substructure.

For the purposes of evaluation and experimentation, it is helpful to point out that: for *Friedif* = 1000, $r.m.s.(D) = 0.1\langle A \rangle$ (i.e. strong differences); for *Friedif* = 100, $r.m.s.(D) = 0.01\langle A \rangle$ (i.e. medium differences); for *Friedif* = 10, $r.m.s.(D) = 0.001\langle A \rangle$ (i.e. weak differences). According to this scale, strong and medium differences are always significant and Friedel's (1913) law only becomes a very good approximation for very weak Friedel differences around *Friedif* = 1. Whilst on such topics, we point out that we much prefer the term *resonant scattering* to those of *anomalous scattering* and *anomalous dispersion* in taking seriously Creagh's (1999) comment that ... *there is nothing anomalous about these corrections. In fact the scattering is totally predictable.*

3. Properties of the Bijvoet intensity ratio

For the study of the properties of the Bijvoet ratio, the data for structures presented in Table 3 were taken from our own structure determinations and also from selected analyses

Table 3

Structures used in the Bijvoet ratio tests.

REFCODE is either that of the CSD or a local code beginning with 9. The only structures for which checkCIF/*PLATON* indicated a quantitative misfit to a centrosymmetric structure were METWIS (88%) and 9YAN01 (87%). Fuller information on these structures and the interpretation of their data is available from the supplementary material.

REFCODE	Space group†	Flack parameter	Reference
CICYIX	<i>aP1</i>	−0.002 (17)	V in Yasodha <i>et al.</i> (2007)
METWIS	<i>aP1</i>	0.010 (10)	Li <i>et al.</i> (2007)
SEZPUJ	<i>aP1</i>	0.12 (11)	Moskalev <i>et al.</i> (2007)
XICNED	<i>aP1</i>	0.012 (7)	Chantrapromma <i>et al.</i> (2007)
UNEVAK01	<i>aP1</i>	0.02 (10)	Zhu & Jiang (2007)
YIDJIF	<i>aP1</i>	0.041 (5)	Chartrand <i>et al.</i> (2007)
GIHDAD	<i>aP1</i>	0.0620 (10)	Wang <i>et al.</i> (2007)
XIFSIP	<i>aP1</i>	0.00 (5)	Xia <i>et al.</i> (2007)
WIGWUF	<i>aP1</i>	−0.016 (10)	Bekaert <i>et al.</i> (2007)
UDUSIW	<i>aP1</i>	−0.03 (7)	Ghadimi <i>et al.</i> (2007)
9BER01	<i>oP2₁2₁2₁</i>	0.00 (3)	K (2 <i>R</i> , 3 <i>R</i>)H-tartrate, 298 K, Mo $K\alpha$
PEFXII	<i>oP2₁2₁2₁</i>	−0.01 (2)	Kündig <i>et al.</i> (2006)
CICXES	<i>oP2₁2₁2₁</i>	0.015 (8)	Cisnetti <i>et al.</i> (2007)
EZEQAB	<i>oP2₁2₁2₁</i>	−0.03 (11)	(<i>S</i>)-B4S in Chauvin <i>et al.</i> (2004)
TIBCAJ	<i>oP2₁2₁2₁</i>	−0.039 (14)	Scharwitz <i>et al.</i> (2007)
RIHMUR	<i>oP2₁2₁2₁</i>	−0.02 (3)	Abbasi <i>et al.</i> (2007)
9YAN01	<i>oP2₁2₁2₁</i>	−0.01 (3)	Yang <i>et al.</i> (2007)
PIFDOY	<i>oP2₁2₁2₁</i>	0.011 (19)	Fu & Zhao (2007)
SIHDET	<i>oP2₁2₁2₁</i>	−0.02 (8)	King <i>et al.</i> (2007)
CIJWUO	<i>oP2₁2₁2₁</i>	0.41 (3)	Blake <i>et al.</i> (2007)
RIGMAW	<i>oP2₁2₁2₁</i>	−0.02 (6)	Cunico <i>et al.</i> (2007)
CIKCUV	<i>oPna2₁</i>	−0.05 (4)	Guzei <i>et al.</i> (2007)
KEXYOC	<i>mCc</i>	−0.05 (5)	Ia in Wardell <i>et al.</i> (2007)
YIFZAP	<i>mPc</i>	−0.1 (3)	Gowda, Nayak <i>et al.</i> (2007)
RIGHEV	<i>mP2₁</i>	0.05 (3)	Gainsford <i>et al.</i> (2007)
TIBFIU	<i>mP2₁</i>	0.010 (10)	Ma (2007)
EDUZOT	<i>mP2₁</i>	0.04 (6)	Zhang & Zheng (2007)
METSIO	<i>mP2₁</i>	−0.021 (3)	Tooke <i>et al.</i> (2007)
GIHKEO	<i>mC2</i>	−0.018 (12)	Gowda, Usha <i>et al.</i> (2007)
TICFIV	<i>mC2</i>	−0.01 (2)	Cymborowski <i>et al.</i> (2007)

† In the symbol for the space group, the lattice-centring code *P*, *A*, *B*, *C*, *I* or *F* has, in each case, been replaced by the appropriate IUCr approved symbol for the Bravais-lattice type: *aP*, *mP*, *mS* (*mC*, *mA*, *mI*), *oP*, *oS* (*oC*, *oA*, *oB*), *oI*, *oF*, *tP*, *tI*, *hP*, *hR*, *hC*, *cI*, *cF* (de Wolff *et al.*, 1985; Hahn & Looijenga-Vos, 2002). This slight change in nomenclature avoids having to write a preceding triclinic, monoclinic, orthorhombic *etc.*, and also allows the importance of the Bravais-lattice type to be emphasized by appearing naturally as part of the space-group symbol.

which have been published in 2007 in *Acta Crystallographica* Section B, C or E up to mid-August 2007. All had refined values of the Flack parameter $x(u)$ and intensity data (model and observed) were available. The intensity data for each selected structure were then arranged into three classes of reflections: (i) centric reflections, (ii) acentric reflections for which only one member of a Friedel pair had been measured and (iii) Friedel pairs of acentric reflections. For class (iii), values of A , D , $u(A)$ and $u(D)$ were calculated.

The standard uncertainties $u(A)$ and $u(D)$ of $A(hkl)$ and $D(hkl)$ and their mutual-uncertainty coefficient $g(AD)$ (akin to a correlation coefficient) are calculated by applying standard propagation of uncertainty formulae to $u[I(hkl)] = u_+$ and $u[I(\bar{h}\bar{k}\bar{l})] = u_-$ assuming the mutual-uncertainty coefficient of $I(hkl)$ and $I(\bar{h}\bar{k}\bar{l})$ to be zero. This gives $4u^2(A) = u^2(D) = (u_+^2 + u_-^2)$ and $g(AD) = (u_+^2 - u_-^2)/(u_+^2 + u_-^2)$.

For each compound presented in Table 3, several values of the Bijvoet ratio were calculated and their numerical values are presented in Table 4. Similarly, Table 5 contains reflection

Table 4

Bijvoet ratio values.

The definition of the various ratios may be found in the glossary. $u > 0$ in the column $10^4\chi_{\text{Oas}}$ means that $\langle u^2 \rangle > \langle D_{\text{Oa}}^2 \rangle$ and the evaluation of $10^4\chi_{\text{Oas}}$ leads to the square root of a negative quantity. CIJWUO is twinned by inversion and $10^4\chi_{\text{Ex}}$ gives values for the untwinned and twinned crystals. Fuller information on these structures and the interpretation of their data is available from the supplementary material.

REFCODE	$10^4\chi_{\text{Ex}}$	$10^4\chi_{\text{Ma}}$	$10^4\chi_{\text{Mz}}$	$10^4\chi_{\text{Oa}}$	$10^4\chi_{\text{Oz}}$	$10^4\chi_{\text{Oas}}$
CICYIX	306	418	217	668	512	$u > 0$
METWIS	575	346	85	417	115	$u > 0$
SEZPUJ	81	128	16	1249	-115	740
XICNED	415	758	281	874	342	394
UNEVAK01	70	175	49	1171	409	623
YIDJIF	693	1084	375	1422	669	712
GIHDAD	792	1099	296	1123	301	522
XIFSIP	104	278	87	1067	411	313
WIGWUF	926	1675	615	1890	594	1548
UDUSIW	74	199	64	907	253	$u > 0$
9BER01	174	537	144	917	301	773
PEFXII	857	625	27	1709	331	1134
CICXES	389	980	379	1135	331	715
EZEQAB	87	468	20	521	30	$u > 0$
TIBCAJ	1220	1768	1005	2054	918	1706
RIHMUR	191	323	61	554	113	468
9YAN01	618	718	183	1442	-628	$u > 0$
PIFDOY	538	531	165	1125	408	440
SIHDET	76	198	72	1032	-145	$u > 0$
CIJWUO	786/126	222	115	1329	77	1000
RIGMAW	89	277	75	1605	-1178	$u > 0$
CIKCUV	120	332	76	492	128	159
KEXYOC	110	299	104	874	173	$u > 0$
YIFZAP	100	474	-48	2787	-298	2762
RIGHEV	248	445	167	1079	-52	687
TIBFIU	486	-	-	551	-	$u > 0$
EDUZOT	109	363	50	1135	109	697
METSIO	1306	1477	768	1804	666	1529
GIHKEO	939	2009	410	2465	543	2323
TICFIV	365	643	205	816	222	736

counts and various estimates of the fit between observed and model values. Tables 3, 4 and 5 contain the same compounds arranged in the same order, the REFCODE of each compound providing the necessary link between the three tables. Looking at Table 4, we find that the expected value of the Bijvoet ratio labelled $10^4\chi_{\text{Ex}}$ is *Friedif*, χ_{M} , and χ_{O} , with some character in place of the \cdot , indicate values calculated respectively from the model and observed intensities of Friedel pairs by using equation (3). Two values are given for each. The first, χ_{a} , is obtained by using all reported Friedel pairs. The second χ_{z} is the value extrapolated to $\sin \theta/\lambda = 0$ and was calculated in a manner similar to that described in §3.1 arranging the limits of $\sin \theta/\lambda$ so as to always have ~ 10 bins. The complete list of Bijvoet ratio symbols may be found in the glossary.

3.1. $\sin \theta/\lambda$ dependence

Flack & Shmueli (2007) have discussed theoretically the dependence on $\sin \theta/\lambda$ of the Bijvoet intensity ratio due to the atomic scattering factors and isotropic atomic displacement parameters. Here we present results from our experimental study of K (2*R*,3*R*)H-tartrate at 298 K measured with Mo *K* α radiation (compound 9BER01 in Tables 3, 4 and 5 and Figs. 4, 5 and 6). Following a least-squares refinement on the whole set

of intensity data, values of $10^4\chi$ were calculated both from the model (calculated) and observed intensities progressively increasing the limit on $\sin \theta/\lambda$ of the reflections included in the sums to take in an extra 100 reflections at a time giving approximately 10 bins in all. Obviously, centric and unpaired acentric reflections were not used in this evaluation. The result is shown in Fig. 4. We concentrate our attention on $10^4\chi_{\text{M}}$, as this contains no random and systematic measurement uncertainties and should be comparable to the value obtained from the Flack & Shmueli (2007) formula. $10^4\chi_{\text{M}}$ is essentially linearly dependent on $\sin \theta/\lambda$ and has a value calculated over all the Friedel pairs reported in the intensity data ($\sin \theta/\lambda \leq 0.71 \text{ \AA}^{-1}$) of $10^4\chi_{\text{Ma}} = 537$, which is much higher than that of *Friedif* of 174 (see Table 4). However, the value of *Friedif* calculated from equation (8) of Flack & Shmueli (2007) is strictly valid only at $\sin \theta/\lambda = 0$. Consequently, that value to be compared with *Friedif* is $10^4\chi_{\text{Mz}}$ following an extrapolation back to $\sin \theta/\lambda = 0.0$. From Fig. 4 and Table 4, an extrapolated value of 144 is obtained. The agreement is good in view of the inevitable lack of intensity data at small values of $\sin \theta/\lambda$.

The increase of χ with respect to $\sin \theta/\lambda$ is due to $\langle D^2 \rangle^{1/2}$ and $\langle A \rangle$ having different dependencies on $\sin \theta/\lambda$.

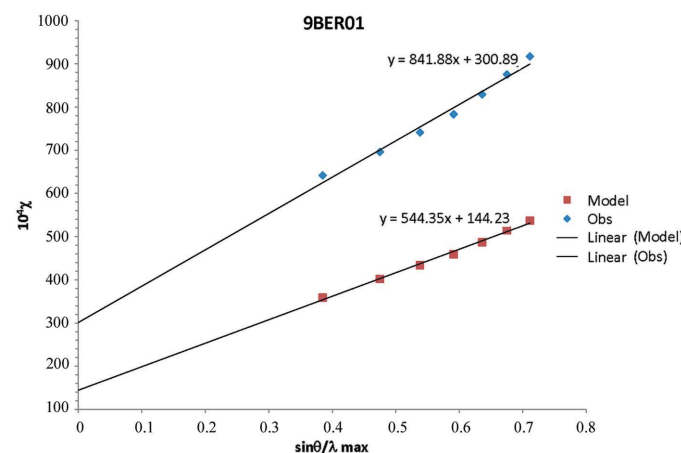


Figure 4
Plot of $10^4\chi$ versus $\sin \theta/\lambda_{\text{max}}$ (\AA^{-1}) for 9BER01.

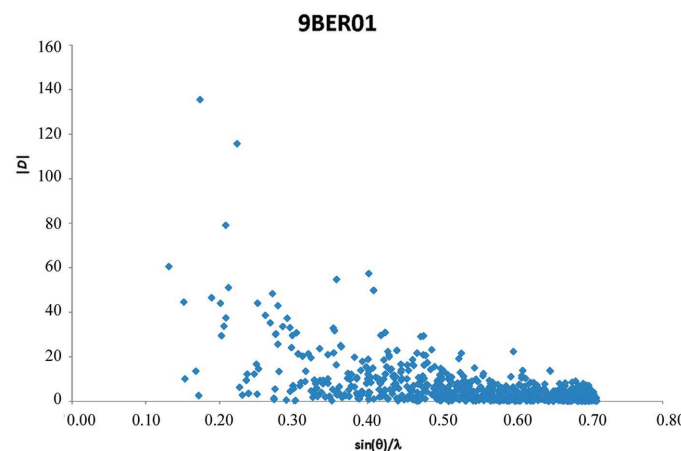


Figure 5
Plot of $|D|$ versus $\sin \theta/\lambda$ (\AA^{-1}) for 9BER01.

Table 5

Bijvoet ratio tests.

Reflection counts and Friedel R factors. The definitions of R_A , R_D , wR_A^2 and wR_D^2 are defined in the *Glossary*. For values of Count presented as $m + n$, m refers to special $0k0$ reflections and n to general hkl reflections. Fuller information on these structures and the interpretation of their data is available from the supplementary material.

REFCODE	Count total	Count pairs	Count centro	Count unpaired	R_A	wR_A^2	R_D	wR_D^2	R.m.s. $\Delta A/u$	R.m.s. $\Delta D/u$	Max $ g(AD) $
CICYIX	2108	1007	0	94	0.032	0.037	0.710	0.619	1.42	0.75	0.89
METWIS	5011	1170	0	2671	0.041	0.053	0.652	0.563	3.03	0.70	0.92
SEZPUJ	7146	335	0	6476	0.063	0.051	1.005	1.006	2.80	1.42	0.67
XICNED	7236	3381	0	474	0.028	0.031	0.527	0.446	1.48	0.71	0.89
UNEVAK01	4322	678	0	2966	0.049	0.059	0.977	0.978	1.73	1.00	0.83
YIDJIF	7003	3134	0	735	0.044	0.053	0.458	0.349	1.58	0.64	0.81
GIHDAD	2423	1078	0	267	0.037	0.045	0.706	0.659	1.13	0.70	0.61
XIFSIP	4860	1046	0	2768	0.043	0.059	0.940	0.937	1.97	0.92	0.92
WIGWUF	1461	658	0	145	0.052	0.065	0.478	0.421	1.98	1.41	0.96
UDUSIW	2791	1328	0	135	0.047	0.061	0.966	0.970	1.68	0.96	0.73
9BER01	1771	738	293	2	0.032	0.037	0.662	0.634	2.10	0.85	0.95
PEFXII	4711	2329	0	30	0.018	0.021	0.848	0.929	0.59	1.31	0.99
CICXES	9372	3880	1013	599	0.041	0.053	0.560	0.526	1.46	0.72	0.86
EZEQAB	4281	2134	0	10	0.012	0.015	0.402	0.492	0.27	0.14	1.00
TIBCAJ	2996	547	625	1277	0.041	0.046	0.628	0.552	1.04	0.98	0.85
RIHMUR	3037	1283	463	8	0.020	0.025	0.725	0.720	2.83	1.59	0.98
9YAN01	1344	488	278	90	0.068	0.077	0.870	0.766	1.22	0.90	0.91
PIFDOY	1884	746	391	1	0.049	0.061	0.815	0.633	1.63	0.95	0.89
SIHDET	6693	2859	953	22	0.076	0.084	0.971	0.973	2.17	0.92	0.93
CIJWUO	3511	414	709	1974	0.055	0.049	0.983	0.993	1.67	1.50	0.12
RIGMAW	6032	2609	735	79	0.071	0.055	0.982	0.977	1.16	0.84	0.98
CIKCUV	2442	1149	142	2	0.037	0.046	0.782	0.744	4.86	1.53	0.92
KEXYOC	2394	1086	12	210	0.048	0.054	0.922	0.894	1.86	0.94	0.93
YIFZAP	1053	378	6	291	0.082	0.072	1.014	0.963	8.64	4.92	0.76
RIGHEV	15832	13 + 7524	289	469	0.085	0.096	0.946	0.940	3.27	1.23	0.91
TIBFIU	3353	1529	98	197	0.074	0.104	–	–	4.34	–	0.94
EDUZOT	1839	854	53	78	0.031	0.045	0.972	0.909	2.48	1.33	1.00
METSIO	28340	10 + 13637	1020	26	0.036	0.034	0.571	0.407	1.28	0.97	0.95
GIHKEO	1879	4 + 784	173	130	0.043	0.044	0.527	0.414	3.11	1.76	0.99
TICFIV	4678	4 + 2138	368	26	0.030	0.041	0.541	0.552	2.80	1.26	0.88

decreases less rapidly than $\langle A \rangle$ as $\sin \theta/\lambda$ increases. The increase of χ with $\sin \theta/\lambda$ is hence an artefact and definitely NOT an indication that the root-mean-square Friedel intensity difference increases with $\sin \theta/\lambda$. Fig. 5 shows, for the same data set of compound 9BER01, individual values of $|D|$. The largest differences are at low $\sin \theta/\lambda$ and it is these which are important in structure refinement especially for absolute-structure determination. The fact that the variations of $\langle D^2 \rangle^{1/2}$ and $\langle A \rangle$ with $\sin \theta/\lambda$ are different implies that the factors to be used in the calculation of normalized intensities and normalized structure factors are different for D and A . As is well known, the appropriate factor to normalize A is the expected value of $\langle A \rangle$, $\sum f_i^2 + \sum f_i'^2$, so the normalized value A' of A is $A' = A/(\sum f_i^2 + \sum f_i'^2)$ and $\langle A' \rangle = 1$. Likewise, a normalized D' is obtained as $D' = D/[4 \sum \sum (f_i f_j'' - f_j f_i'')^2]^{1/2}$ with $\langle D'^2 \rangle = 1$. We know of no existing practical application of the normalized Friedel difference D' .

3.2. Bijvoet ratios of model intensities

Whether or not the model is a good representation of the real crystal, the two values χ_{Ex} and χ_{M} should be approximately equal. However, we note for most structures that χ_{Ma} is larger or much larger than χ_{Ex} although there are a few cases (*viz* METWIS and PEFXII) where χ_{Ma} is smaller. In general, the graphs of $10^4 \chi$ versus $\sin \theta/\lambda$ present the same character-

istics as seen in Fig. 4 showing a strong dependence on $\sin \theta/\lambda$ of χ . It is thus thought preferable to compare χ_{Ex} with χ_{Mz} , the value of χ_{M} extrapolated to $\sin \theta/\lambda = 0$. In all cases, χ_{Mz} is smaller than χ_{Ex} and in the cases of METWIS, SEZPUJ, PEFXII, EZEQAB and YIFZAP considerably smaller. For these latter cases, it may be that χ_{Ex} is too large and has to be reduced to take account of the presence of a centrosymmetric substructure. We have not pursued this analysis further in view of the known difficulties of establishing any valid quantitative measure of pseudo-symmetry (see for example Collins *et al.*, 2006; Rassat & Fowler, 2004; Spek, 2003). For the other structures, there is no indication of a centrosymmetric substructure by checkCIF/PLATON. In view of the inevitable uncertainty in performing the extrapolation of χ_{M} to $\sin \theta/\lambda = 0$, we judge the agreement between χ_{Ex} and χ_{Mz} as satisfactory. Clearly, the comparison of χ_{Ex} and χ_{Ma} is unsatisfactory but understandable in view of the dependence of the Bijvoet intensity ratio on $\sin \theta/\lambda$.

3.3. Symmetry-enhancement factors

The analysis of Flack & Shmueli (2007) is applicable to the triclinic space group $P1$ with a centrosymmetric substructure. It was not at all obvious to us that this analysis could be used *per se* for other non-centrosymmetric space groups. As a consequence, we undertook the work presented by Shmueli *et*

Table 6

Intensity statistics on special and general reflections.

REFCODE	Refns. count	Model (<i>A</i>)	Model r.m.s. <i>D</i>	Obs. (<i>A</i>)	Obs. r.m.s. <i>D</i>
RIGHEV	0 <i>k</i> 0, 13	11206	173	11314	608
	<i>hkl</i> , 4793	2981	121	2988	285
METSIO	0 <i>k</i> 0, 10	240543	11343	216981	29680
	<i>hkl</i> , 12384	13131	1907	13161	2250
TIBFIU	0 <i>k</i> 0, 8	3406	–	3485	78
	<i>hkl</i> , 369	819	–	840	30
GIHKEO	0 <i>k</i> 0, 4	6842	268	6986	420
	<i>hkl</i> , 1917	1517	291	1529	359
TICFIV	0 <i>k</i> 0, 4	12436	203	13119	403
	<i>hkl</i> , 1253	3635	200	3641	248

al. (2008) reporting relevant theoretical intensity statistics for general and special reflections for all non-centrosymmetric space groups. On the practical side, we have used the data sources described in §3 to study ten structure analyses in the triclinic space group *P*1 (*i.e.* compounds CICYIX to UDUSIW inclusive) and a comparable number in the common orthorhombic space group *P*₂₁2₁2₁ (*i.e.* compounds 9BER01 to RIGMAW inclusive) together with some examples in monoclinic space groups *P*₂₁ (*i.e.* compounds RIGHEV to METSIO inclusive) and *C*2 (*i.e.* compounds GIHKEO and TICFIV). Results are given in Table 4. These show, as seen in §3.2, that χ_{Mz} is in reasonable agreement with the value χ_{Ex} , in agreement with Shmueli *et al.*'s (2008) analysis that there is no symmetry-enhancement factor for general reflections in these low-symmetry non-centrosymmetric space groups.

A few further tests were made for symmetry-enhancement factors on special reflections. We chose to study the 0*k*0 reflections in structures in the monoclinic space groups *P*₂₁ and *C*2. From the 2007 *Acta Crystallographica* sources, we selected those structures in these two space groups which had the largest values of the cell parameter *b* (to maximize the number of 0*k*0 reflections) and which had acceptable values of the Flack parameter and its standard uncertainty. The results are given in Table 6 where the statistics on the special 0*k*0 reflections can be compared to those of general *hkl* reflections. With the proviso that the number of 0*k*0 reflections in these structure determinations is very small and does not allow for satisfactory statistics, the main conclusions of Shmueli *et al.* (2008) are upheld. The $\langle A \rangle$ of the special 0*k*0 reflections is considerably larger than that of the general *hkl* reflections and the corresponding $\langle D^2 \rangle^{1/2}$ is also increased. It is not possible to say more from such a small set of data.

3.4. Bijvoet ratios of observed intensities

On consulting the values of χ_O in Table 4, one sees that in general χ_O is larger than χ_M . This is clearly due to the effect of random and systematic uncertainties in the observed intensities. Moreover, for the observed intensities the extrapolation to $\sin \theta/\lambda = 0$ leads to a negative value of χ_{Oz} (six cases) much more frequently than is the case of χ_{Mz} , only one case (YIFZAP). The plots of χ_O versus $\sin \theta/\lambda$ show a greater tendency than those of χ_M to depart from a linear relation-

Table 7

Bijvoet ratio values from centric reflections.

REFCODE	Centro count	$10^4 \chi_{Oc}$	$10^4 \chi_{Oar}$
9BER01	575	1118	727
PEFXII	1186	1555	1521

χ_{Oc} is calculated using intensity data of the centric reflections. χ_{Oar} is the value of χ_{Oa} corrected by use of χ_{Oc} . $u > 0$ means that $\langle u^2 \rangle > \langle D_{Oa}^2 \rangle$ and the evaluation of χ_{Oar} leads to the square root of a negative quantity.

ship, some of them being clearly parabolic. As $\langle D_{Oa}^2 \rangle$ contains contributions both from the real difference in intensity between Friedel opposites (*i.e.* DX_i for the *i*th Friedel pair) and random and systematic uncertainties (*i.e.* e_i for the *i*th Friedel pair), we experimented with two potential ways to correct χ_O for random and systematic uncertainties. In the event, both of these procedures turned out to be unsatisfactory and consequently they are only described succinctly.

In the first procedure, which leads to χ_{Oas} , we use the values of the standard uncertainties of D_i^{obs} as an expression of the random and systematic uncertainties. Writing $D_i^{obs} = DX_i + e_i$ with $e_i = N(0, \sigma_i^2)$, where $N(\mu, \nu)$ indicates a normal distribution of mean μ and variance ν , we obtain $\langle D^2 \rangle = 1/N \sum (DX_i + e_i)^2 = 1/N \sum DX_i^2 + 1/N \sum e_i^2 + 2/N \sum DX_i e_i$. Taking expectations, $E[\langle D^2 \rangle] = \langle DX^2 \rangle + \langle \sigma^2 \rangle$. For practical purposes, one writes $\langle D_{Oas}^2 \rangle = \langle D_{Oa}^2 \rangle - \langle u^2 \rangle$ and uses $\langle D_{Oas}^2 \rangle$ to obtain χ_{Oas} . Comparing χ_{Oa} with χ_{Oas} , we find there are several cases where $\langle u^2 \rangle$ is greater than $\langle D_{Oa}^2 \rangle$ resulting in a square root of a negative quantity appearing in the calculation of χ_{Oas} . In another case (*i.e.* CIKCUV), the value of χ_{Oas} is rather small. For all these cases, it seems that the standard uncertainties of the intensity data are largely overestimated. One notices also that the low values given in Table 5 of the root-mean-square values of $\Delta A/u$ and $\Delta D/u$ confirm this overestimation. An opposing case is YIFZAP for which the difference between χ_{Oa} and χ_{Oas} is very small. The standard uncertainties of the intensity data seem to have been underestimated in this case.

In the second procedure, which leads to χ_{Oar} , we make use of the intensity data of centric reflections indicated in Table 3 of Shmueli *et al.* (2008). These are ones for which $I(hkl)_{model} = I(\bar{h}\bar{k}\bar{l})_{model}$ for specific classes of reflection depending on the geometric crystal class of the crystal (*e.g.*, for the orthorhombic space group *P*₂₁2₁2₁, 0*kl*, *h*0*l* and *hk*0 are centric reflections). In practice, using standard averaging software, in order not to merge $I(hkl)$ and $I(\bar{h}\bar{k}\bar{l})$, one has to work in space group *P*1 for these centric reflections whereas the acentric reflections are treated normally in the space group of the crystal structure. The $D(hkl)$ of centric reflections contain only the contribution of random and systematic uncertainties in the intensity data. Letting *M* be the number of symmetry-equivalent general reflections (*e.g.* in *P*₂₁2₁2₁, *M* = 4), one obtains $\langle D_{Oar}^2 \rangle = \langle D_{Oa}^2 \rangle - (1/M) \langle D_{Oc}^2 \rangle$. The factor of 1/*M* arises in the following way. If ε is a random variable distributed like $N(0, \sigma^2)$ and $\kappa = 1/M \sum \varepsilon_i$, then κ is distributed like $N(0, \sigma^2/M)$. The intensities of centric reflections are unaveraged whereas the intensities of acentric reflections are obtained by averaging *M* intensities. Turning to Table 7, one

sees that for 9BER01 the unaveraged centric reflections seem to have provided a satisfactory correction for random and systematic effects in the intensity data. However, for PEFXII the correction is unsatisfactory. More tests are required but the intensity data available with structure determinations in *Acta Cryst.* B, C and E are unsuitable as they have already been averaged in the crystal point group resulting in the loss of the $D(hkl)$ for the centric reflections necessary for this calculation. A further limitation of this correction is that centric reflections are in short supply in low-symmetry space groups (*i.e.* none in geometric class 1, only $0k0$ in m , only $h0l$ in 2, only $hk0$ in $mm2$ but $0kl$, $h0l$ and $hk0$ in 222), see Shmueli *et al.* (2008, Table 3).

The above results show that, in practice, our two proposed methods for correcting χ_O do not give reliable results. This is most unfortunate as for the purposes of data evaluation χ_O would be preferable to χ_M as it does not in any way depend on a structural model being available.

3.5. Quality of intensity data and fit

If we refer to Table 5, it comes as somewhat of a surprise that there are often a large number of acentric reflections for which the intensity of the Friedel opposite is not available. It is not at all clear why this should be or why a data-measurement strategy leading to a large number of unpaired Friedel opposites should have been chosen. We hence suggest that a good way of judging the quality of an intensity data set of a non-centrosymmetric crystal structure is to count and report the number of unpaired acentric reflections as a complement to the numbers of measured acentric pairs and measured centric reflections. Moreover, we have also examined the values of the A to D mutual-uncertainty coefficient $g(AD)$ as defined above in §3. Small values of $|g(AD)|$ mean that the standard uncertainties of $I(hkl)_{\text{obs}}$ and $I(\bar{h}\bar{k}\bar{l})_{\text{obs}}$ are approximately equal, whereas values of $|g(AD)|$ close to unity mean that one of $I(hkl)_{\text{obs}}$ and $I(\bar{h}\bar{k}\bar{l})_{\text{obs}}$ has been measured with a far greater uncertainty than the other. Consequently, the largest absolute value of the AD mutual-uncertainty coefficient,

$|g(AD)|_{\text{max}}$, is a good guide to the homogeneity of the data collection. So although for routine structure analysis it might be considered satisfactory merely to have intensity measurements of a sufficiently large number of Friedel opposites, we consider that, for accurate electron-density measurements and absolute-configuration determination of low-*Friedel* compounds, the number of unpaired Friedel opposites should be very small and a value of $|g(AD)|_{\text{max}}$ which is close to zero should be a requirement. For compound 9BER01, we examined scatter diagrams of $|g(AD)|$ versus $\sin \theta/\lambda$, $|g(AD)|$ versus A and $|g(AD)|$ versus $|D|$ but these do not show any apparent relationships between the variables considered.

Concerning the measures of the least-squares fit of the data to the model, examination of the Friedel R factors and root-mean-square deviates in Table 5 is instructive. The $A(hkl)$ are being better fit than the $D(hkl)$. Although the R values clearly show that A is being better fit than D , the root-mean-square $\Delta D/u$ and $\Delta A/u$ seem to indicate that the goodness of fits of D and A are comparable although in general that of D is smaller than that of A . However, on closer inspection one sees that the $u(A)$ and $u(D)$ are essentially identical whereas $|D|$ is much smaller than A . Thus, $|\Delta D|$ should be much smaller than $|\Delta A|$ and the root-mean-square value of $\Delta D/u$ should be much smaller than that of A . Hence the observed root-mean-square value of $\Delta D/u$, although it looks small and acceptable, is in fact much larger than it should be and is unacceptable in the same way as the R factors of D . The vast majority of the values of root-mean-square $\Delta A/u$ are in a range $1.0 \leq \text{r.m.s.}(\Delta A/u) \leq 3.0$ expected of a satisfactory goodness of fit. It is however very difficult to escape from an overbearing impression that these are no more than target values obtained by some empirical parameterization of the standard uncertainties of the intensities rather than properly indicating any real statistical property of the data and their fit to the model.

3.6. Classes of reflections with large $|D|$

For the planning of experiments, it is useful to know for an unknown crystal structure whether there are regions of reciprocal space where larger than average values of $|D|$ may be found. It has already been seen in §3.3 and Shmueli *et al.* (2008) that special reflections have increased values of the root-mean-square Friedel difference. The appropriate special reflections may be found in Table 3 of Shmueli *et al.* (2008) by seeking the largest values of $\langle D^2 \rangle^{1/2}/\rho$ for the space group under consideration. Unfortunately, the number of enhanced reflections tends to be rather small. In passing, it should be noted that centric reflections have a value of $\langle D^2 \rangle^{1/2}/\rho = 0$ in this table. It has already been seen in §3.1 and Fig. 5 that reflections with large $|D|$ tend to lie at low $\sin \theta/\lambda$. Examination of Fig. 6 for the same compound shows that an empirical linear relationship exists between $|D|$ and A , so roughly the reflections of strongest intensity will on average have the largest absolute value of the Friedel intensity difference. Consequently and regrettably, those reflections which tend to have a large absolute value of the Friedel-intensity difference are exactly those likely to suffer from the effects of extinction.

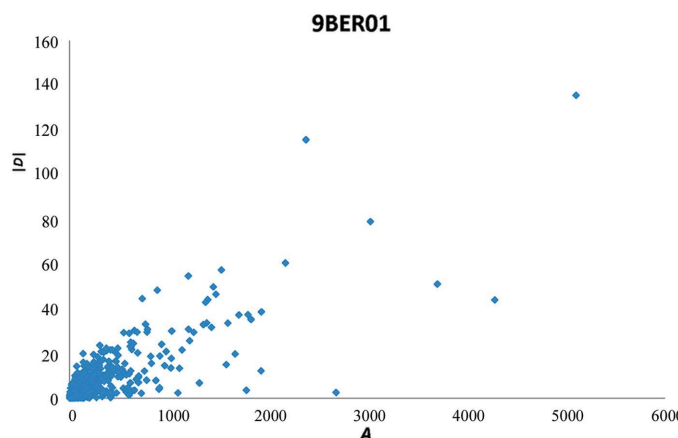


Figure 6
Plot of $|D|$ versus A for 9BER01.

Plots of $|D|$ versus $\sin \theta/\lambda$ and $|D|$ versus A are available in the supplementary material for all compounds in Tables 3, 4 and 5.² They all show exactly the same characteristics as 9BER01. In this and other respects, 9YAN01 is the compound which differs the most from the rest. It has large values of $|D|$ out to higher values of $\sin \theta/\lambda$ than the others, and also shows large values of $|D|$ for small values of A and small values of $|D|$ for large values of A . 9YAN01 is the only non-molecular compound in our data sets and contains no C atoms (hence it does not have a CSD refcode). It is of the mineral cobalt-austinite $\text{CaCo}(\text{AsO}_4)(\text{OH})$.

4. Software

Values of *Friedif* were calculated with the spreadsheet application for Microsoft Excel[™] 2003/2007 described in Flack & Shmueli (2007). The software has been extended to allow the calculation with Cr $K\alpha$ radiation as well as Cu $K\alpha$ and Mo $K\alpha$. The calculation of the value *Rescat* of Girard *et al.* (2003) has been removed. The current version of the software is available as extra supplementary material to Flack & Shmueli (2007). The values obtained from the spreadsheet have been verified by extensive hand calculations.

5. Concluding remarks

Our previous (Flack & Shmueli, 2007; Shmueli *et al.*, 2008) and current work clearly show some of the theoretical and practical advantages of dealing with average and difference Friedel intensities in place of the native $I(hkl)$ and $I(\bar{h}\bar{k}\bar{l})$. Further developments are to be expected. It is to be noted that, in *FULLPROF* (Rodriguez-Carvajal, 2005), a very widely used Rietveld refinement software for powder diffraction data, the calculation of intensities and their derivatives is undertaken directly in terms of $A(hkl)$, the quantity observed in powder diffraction, rather than the individual (unobserved) $I(hkl)$ and $I(\bar{h}\bar{k}\bar{l})$. The $D(hkl)$ cannot be observed (or interpreted) in a powder diffraction experiment and consequently it is not necessary to calculate these values.

At a time when resonant scattering with its numerous proven applications is the rule rather than the exception, it seems anachronistic in many basic presentations of X-ray structure analysis to find Friedel's law (Friedel, 1913) being used as a simplifying assumption. Standard presentations (*e.g.* Looijenga-Vos & Buerger, 2002) of point-group and space-group determination all justify the use of Laue classes, even for non-centrosymmetric crystals, by invoking Friedel's law as a reasonably valid assumption. A more modern approach, without approximation and valid for both centrosymmetric and non-centrosymmetric crystals, would be to describe the same analysis as being based on the properties of the average Friedel intensity $A(hkl)$. The symmetry of $A(hkl)$ necessarily belongs to one of the Laue classes [*i.e.* the point group of the

$I(hkl)$ augmented by the inversion operator] without reliance on Friedel's law. The analysis of the $D(hkl)$, which has the 'anti-point-group' symmetry [*i.e.* the point group of the $I(hkl)$ augmented by the property $D(hkl) = -D(\bar{h}\bar{k}\bar{l})$] uncovers extra information.

6. Glossary

$A = A(hkl) = \frac{1}{2}[I(hkl) + I(\bar{h}\bar{k}\bar{l})]$: the average Friedel intensity
 $D = D(hkl) = I(hkl) - I(\bar{h}\bar{k}\bar{l})$: the difference Friedel intensity

$\Delta A = A_{\text{obs}} - A_{\text{model}}$

$\Delta D = D_{\text{obs}} - D_{\text{model}}$

$\chi = \langle D^2 \rangle^{1/2} / \langle A \rangle$: the Bijvoet intensity ratio

χ_{Ex} the expected value of the Bijvoet intensity ratio calculated by using equation (8) of Flack & Shmueli (2007)

χ_{Ma} Bijvoet intensity ratio calculated from model intensities of all reported Friedel pairs

χ_{Mz} Bijvoet intensity ratio calculated from model intensities of reported Friedel pairs extrapolated to $\sin \theta/\lambda = 0$

χ_{Oa} Bijvoet intensity ratio calculated from observed intensities of all reported Friedel pairs

χ_{Oz} Bijvoet intensity ratio calculated from observed intensities of reported Friedel pairs extrapolated to $\sin \theta/\lambda = 0$

χ_{Oas} Bijvoet intensity ratio calculated from observed intensities of all reported Friedel pairs and corrected for random and systematic uncertainties by using the reported standard uncertainties of the observed intensities

χ_{Oc} Bijvoet intensity ratio calculated from observed intensities of unaveraged Friedel pairs of centric reflections

χ_{Oar} Bijvoet intensity ratio calculated from observed intensities of all reported Friedel pairs and corrected for random and systematic uncertainties by using χ_{Oc}

$Friedif = 10^4 \chi_{\text{Ex}}$

$R_A = \sum(|A_{\text{obs}} - A_{\text{model}}|) / \sum(|A_{\text{obs}}|)$: conventional R factor for A

$R_D = \sum(|D_{\text{obs}} - D_{\text{model}}|) / \sum(|D_{\text{obs}}|)$: conventional R factor for D

$wR_A^2 = \{\sum[(A_{\text{obs}} - A_{\text{model}})/u(A_{\text{obs}})]^2 / \sum[A_{\text{obs}}/u(A_{\text{obs}})]^2\}^{1/2}$: weighted R factor for A

$wR_D^2 = \{\sum[(D_{\text{obs}} - D_{\text{model}})/u(D_{\text{obs}})]^2 / \sum[D_{\text{obs}}/u(D_{\text{obs}})]^2\}^{1/2}$: weighted R factor for D

u the standard uncertainty of the cited quantity

$g(AD)$ the mutual-uncertainty coefficient of A and D

Dr M. Hoyland of the IUCr Research and Development group is thanked for providing a list of structures published in 2007 in *Acta Crystallographica* Sections B, C and E containing numerical values of the Flack parameter.

² These data are available from the IUCr electronic archives (Reference: SH5074). Services for accessing these archives are described at the back of the journal.

References

- Abbasi, A., Habibian, M. & Sandström, M. (2007). *Acta Cryst.* **E63**, m1904.
- Bekaert, A., Lemoine, P., Brion, J. D. & Viossat, B. (2007). *Acta Cryst.* **E63**, o3187–o3189.
- Blake, A. J., Lippolis, V., Pivetta, T. & Verani, G. (2007). *Acta Cryst.* **C63**, m364–m367.
- Chantrapromma, S., Jindawong, B., Fun, H.-K. & Patil, P. S. (2007). *Acta Cryst.* **E63**, o2321–o2323.
- Chartrand, D., Theobald, I. & Hanan, G. S. (2007). *Acta Cryst.* **E63**, m1561.
- Chauvin, A.-S., Bernardinelli, G. & Alexakis, A. (2004). *Tetrahedron Asymmetry*, **15**, 1857–1879.
- Cisnetti, F., Guillot, R., Thérissod, M. & Polcar, C. (2007). *Acta Cryst.* **C63**, m201–m203.
- Clemente, D. A. (2007). Personal communication.
- Collins, A., Cooper, R. I. & Watkin, D. J. (2006). *J. Appl. Cryst.* **39**, 842–849.
- Creagh, D. C. (1999). *International Tables for Crystallography*, Vol. C, *Mathematical, Physical and Chemical Tables*, edited by A. J. C. Wilson & E. Prince, Section 4.2.6. Dordrecht: Kluwer Academic Publishers.
- Cunico, W., Gomes, C. R. B., Wardell, S. M. S. V., Low, J. N. & Glidewell, C. (2007). *Acta Cryst.* **C63**, o411–o414.
- Cymborowski, M., Chruszcz, M., Dauter, Z. & Minor, W. (2007). *Acta Cryst.* **E63**, o1557–o1559.
- Djukic, J.-P., Hijazi, A., Flack, H. D. & Bernardinelli, G. (2008). *Chem. Soc. Rev.* **37**, 406–425.
- Ermer, O. & Dunitz, J. D. (1970). *Acta Cryst.* **A26**, 163.
- Flack, H. D. (1983). *Acta Cryst.* **A39**, 876–881.
- Flack, H. D. & Bernardinelli, G. (1999). *Acta Cryst.* **A55**, 908–915.
- Flack, H. D. & Bernardinelli, G. (2000). *J. Appl. Cryst.* **33**, 1143–1148.
- Flack, H. D. & Bernardinelli, G. (2006). *Inorg. Chim. Acta*, **359**, 383–387.
- Flack, H. D. & Bernardinelli, G. (2008). *Chirality*, **20**, 681–690.
- Flack, H. D., Bernardinelli, G., Clemente, D. A., Linden, A. & Spek, A. L. (2006). *Acta Cryst.* **B62**, 695–701.
- Flack, H. D. & Shmueli, U. (2007). *Acta Cryst.* **A63**, 257–265.
- Friedel, G. (1913). *C. R. Acad. Sci. Paris*, **157**, 1533–1536.
- Fu, D.-W. & Zhao, H. (2007). *Acta Cryst.* **E63**, m1630.
- Gainsford, G. J., Lensink, C. & Falshaw, A. F. (2007). *Acta Cryst.* **C63**, m331–m334.
- Ghadimi, S., Valmoozi, A. A. E. & Pourayoubi, M. (2007). *Acta Cryst.* **E63**, o3260.
- Girard, É., Stelter, M., Vicat, J. & Kahn, R. (2003). *Acta Cryst.* **D59**, 1914–1922.
- Gowda, B. T., Nayak, R., Kožíšek, J., Tokarčík, M. & Fuess, H. (2007). *Acta Cryst.* **E63**, o2967.
- Gowda, B. T., Usha, K. M., Kožíšek, J., Tokarčík, M. & Fuess, H. (2007). *Acta Cryst.* **E63**, m1739–m1740.
- Guzei, I. A., Keter, F. K., Spencer, L. C. & Darkwa, J. (2007). *Acta Cryst.* **C63**, o481–o483.
- Hahn, Th. & Looijenga-Vos, A. (2002). *International Tables for Crystallography*, Vol. A, *Space-Group Symmetry*, edited by Th. Hahn, Table 2.1.2.1. Dordrecht: Kluwer Academic Publishers.
- King, G., Bergin, E., Müller-Bunz, H. & Gilheany, D. G. (2007). *Acta Cryst.* **E63**, o3278.
- Kündig, E. P., Datta Chaudhuri, P., House, D. & Bernardinelli, G. (2006). *Angew. Chem. Int. Ed.* **45**, 1092–1095.
- Levenberg, K. (1944). *Q. Appl. Math.* **2**, 164–168.
- Li, H.-Y., Huang, F.-P., Jiang, Y.-M. & Ng, S. W. (2007). *Acta Cryst.* **E63**, m219–m220.
- Looijenga-Vos, A. & Buerger, M. J. (2002). *International Tables for Crystallography*, Vol. A, *Space-Group Symmetry*, edited by Th. Hahn, ch. 3, pp. 43–54. Dordrecht: Kluwer Academic Publishers.
- Ma, A.-Q. (2007). *Acta Cryst.* **E63**, m1073–m1075.
- Marquardt, D. W. (1963). *SIAM J. Appl. Math.* **11**, 431–441.
- Marsh, R. E. (1981). *Acta Cryst.* **B37**, 1985–1988.
- Marsh, R. E. (1986). *Acta Cryst.* **B42**, 193–198.
- Moskalev, N. V., Gribble, G. W. & Jasinski, J. P. (2007). *Acta Cryst.* **E63**, o1279–o1281.
- Rassat, A. & Fowler, P. W. (2004). *Chem. Eur. J.* **10**, 6575–6580.
- Rodriguez-Carvajal, J. (2005). *FULLPROF Suite*, LLB Saclay and LCSIM Rennes, France.
- Scharwitz, M., Schäfer, S., van Almsick, T. & Sheldrick, W. S. (2007). *Acta Cryst.* **E63**, m1111–m1113.
- Shmueli, U., Schiltz, M. & Flack, H. D. (2008). *Acta Cryst.* **A64**, 476–483.
- Spek, A. L. (2003). *J. Appl. Cryst.* **36**, 7–13.
- Tooke, D. M., Zipp, E. J., van der Vlugt, J. I., Vogt, D. & Spek, A. L. (2007). *Acta Cryst.* **E63**, m86–m88.
- Wang, B.-T., Luo, S.-P., Yue, H.-D., Wang, L.-P. & Xu, D.-Q. (2007). *Acta Cryst.* **E63**, o2786.
- Wardell, S. M. S. V., de Souza, M. V. N., Wardell, J. L., Low, J. N. & Glidewell, C. (2007). *Acta Cryst.* **B63**, 101–110.
- Watkin, D. (1994). *Acta Cryst.* **A50**, 411–437.
- Wolff, P. M. de, Belov, N. V., Bertaut, E. F., Buerger, M. J., Donnay, J. D. H., Fischer, W., Hahn, Th., Koptsik, V. A., Mackay, A. L., Wondratschek, H., Wilson, A. J. C. & Abrahams, S. C. (1985). *Acta Cryst.* **A41**, 278–280.
- Xia, C.-N., Li, B.-W., Hu, W. & Zhou, W. (2007). *Acta Cryst.* **E63**, o3107.
- Yang, H., Costin, G., Keogh, J., Lu, R. & Downs, R. T. (2007). *Acta Cryst.* **E63**, i53–i55.
- Yasodha, V., Govindarajan, S., Low, J. N. & Glidewell, C. (2007). *Acta Cryst.* **C63**, m207–m215.
- Zhang, C.-N. & Zheng, Y.-F. (2007). *Acta Cryst.* **E63**, o3310.
- Zhu, H.-Y. & Jiang, S.-D. (2007). *Acta Cryst.* **E63**, o2833.